Visible to Near-infrared Chip-integrated Tunable Optical Modulators Based on Niobium Plasmonic Nano-antenna and Nano-circuit Metasurface Arrays

Kaveh Delfanazari[1] and Otto L. Muskens[2]

[1]James Watt School of Engineering, University of Glasgow, Glasgow G12 8QQ, UK
[2]Physics and Astronomy, University of Southampton, Southampton SO17 1BJ, UK

Abstract— We report on the numerical and experimental demonstration of novel chip-integrated tunable optical modulators operating at visible to near-infrared telecommunication bands. Our integrated photonic devices are based on plasmonic nano-antenna and nano-circuit metasurface arrays fabricated on the facet of niobium (Nb) thin metallic films. We engineer the photoresponse of our Nb nano-antenna based modulator devices and observe optical modulation properties with a modulation depth MD $\cong$ 60% at $\lambda = 716\,\text{nm}$, and a maximum extinction $A(\lambda) = 1 - R(\lambda) \cong 95\%$ at $\lambda = 650\,\text{nm}$, at room temperature. Moreover, with a similar photoresponse engineering technique, we observe a maximum extinction $A(\lambda) \cong 88\%$ at $\lambda = 1380\,\text{nm}$ in our near-infrared nano-circuit array-based modulators. Our optical modulators are polarization-sensitive, and their photoresponse can be controlled by altering the geometrical parameters of their subwavelength elements and unit cells. Our ultracompact Nb modulators, with their tunable and controllable photoresponse, empower new types of optical links and photonic interconnects interfacing quantum circuits and fibre optic telecommunication systems for applications in quantum technologies.

1. INTRODUCTION

Superconducting-based quantum circuits have demonstrated capability as a primary technology for quantum computing [1–5]. Cryogenic photonic interconnects utilizing optical fibres with their low thermal conductivity have been demonstrated recently to overcome the issue with heat load related to the quantum processors scale up in the dilution refrigerators. Such devices are also capable of connecting superconducting quantum hardware nodes with fibre-based telecommunication platforms [6–8]. Superconducting nano-junctions and nano-devices are the most important part of superconducting quantum technology. They have a wide range of applications, from Andreev devices to superconducting quantum interference devices (SQUIDs) to superconducting nanowire single-photon detectors to superconducting qubits to coherent light sources and ultrasensitive detectors, etc. [1–31]. However, the photoresponse of most superconducting quantum circuits elements, especially of their material building blocks and the materials interfacing superconducting quantum hardware and telecommunication photonic circuits, their suitability and performance are yet to be examined and explored [9, 10].

Here, as the initial stage, we use a microspectrophotometer and ultrafast lasers and investigate the optical properties of unstructured niobium (Nb) thin films. We then proceed by using nanofabrication techniques, and demonstrate optical modulators based on nanostructures such as nano-antenna arrays, nano-split ring resonators arrays and nano-circuit arrays of diverse geometries, nanofabricated on the facet of Nb thin films. We manufactured our ultracompact nanostructure arrays by sputtering a 300 nm Nb thin film on a half-millimetre thick sapphire substrate. We made five chips, each consisting of an array of Nb nanostructures, each comprising an overall area of $100 \times 100\,\mu\text{m}^2$. The photoresponse of our nano-devices can be modulated in two different ways: (i) by altering the dimensions of their subwavelength nanoscale elements and unit cells (the focus of this work). (ii) by changing temperature, considering that metallic Nb switches to superconducting quantum mechanical phases below $T_c \cong 9\,\text{K}$, our nano-device arrays switch from a lossy metallic to low-loss quantum mechanical states close and below their superconducting transition temperature (results to be presented elsewhere).

2. RESULTS

2.1. Optical Modulator Metasurface Nano-devices for Visible-light Telecommunication Band

All five chips were nanofabricated by employing a focused ion beam (FIB) (FEI Helios NanoLab 600) in the facet of thin Nb film, as shown in Fig. 1(a) for nano-slit arrays and Fig. 1(c) for

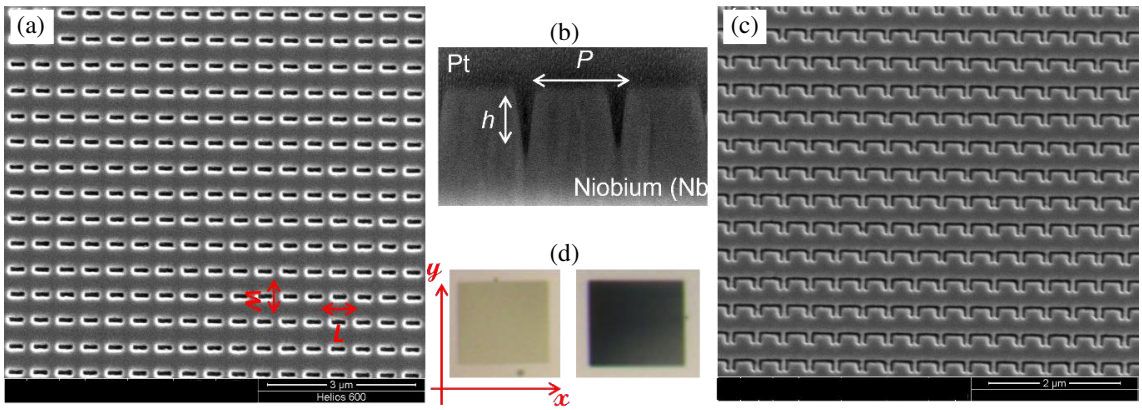

Figure 1: Chip-integrated optical modulators with Nb plasmonic nanoantenna arrays for visible telecommunication band: (a) Scanning Electron Microscope (SEM) image of the ultracompact nano-antenna arrays nanofabricated on the facet of thin Nb films with a thickness of 300 nm. (b) The cross section of the nanoantenna element with a period of $P = 500$ nm and a depth of $h \cong 200$ nm. For such characterisation purposes, Platinum (Pt) layer was deposited for protection throughout sectioning. (c) SEM image of the ultracompact nano-split ring resonator metasurface arrays nanofabricated on the facet of thin Nb film with a thickness of 300 nm. (d) Plasmonic colours for the arrays are shown for two different incident light polarizations P_x (left) and P_y (right).

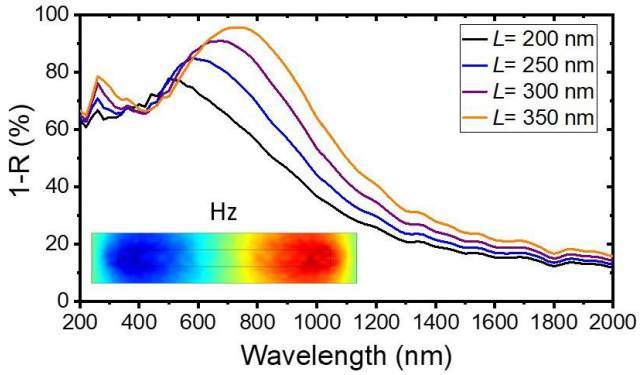

Figure 2: Photo-response of the optical modulators based on Nb nano-antenna arrays in the visible-light telecommunication band: The extinction spectra as a function of wavelength calculated by using COMSOL numerical simulation for four nano-antennas array chips with length $L = 200$ nm, 250 nm, 300 nm, and 350 nm for light polarized perpendicular to the nano-slits arrays. The width is fixed to $w = 50$ nm for all devices inset is the Hz in the nano-antenna at $\lambda = 650$ nm (COMSOL).

nano-split ring resonator arrays. The high fabrication quality and uniformity of the samples were confirmed by scanning electron microscope (SEM) images. Fig. 1(b) is a cross-section of the array element showing a slit profile with period $P = 500$ nm and an average depth $h = 200$ nm.

We fabricated four chips with an array of nano-antennas (slits). The lengths of the slits from chip to chip varied between $L = 200$ nm and 350 nm with a step of 50 nm. The width of the nano-slits in all devices was fixed to be $w = 50$ nm. Figs. 2 and 3 demonstrate a good agreement between the COMSOL numerical simulations and experimental results taken by using a microspectrophotometer, respectively. The dark-yellow graph in Fig. 3 shows the extinction spectra as a function of wavelength for unstructured thin Nb film for perpendicular polarized light. We find that unstructured thin Nb film doesn't offer a strong photoresponse [9].

On the contrary, we observe a strong photoresponse and narrow plasmon resonances that are modulated by the subwavelength geometrical parameters of the nano-antenna arrays for light polarized perpendicular to the chip plane, at room temperature. Such plasmonic resonances were also found to be strongly polarization-dependent, and they disappear for horizontally polarized light (not shown here) [9]. Plasmonic colours for the Nb modulators based on nano-split ring resonator arrays are shown in Fig. 1(d) for two different incident light polarizations, P_x (left) and P_y (right).

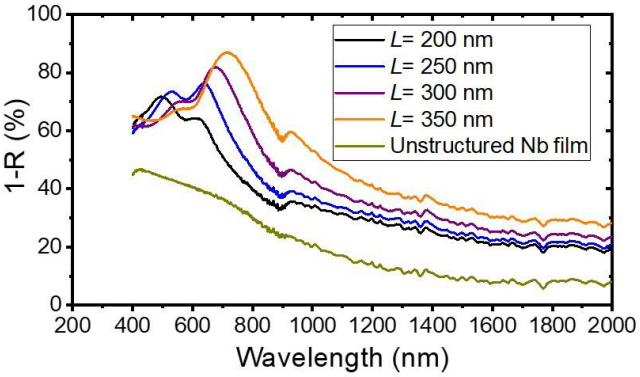

Figure 3: Photo-response of the optical modulators based on Nb nano-antenna arrays in the visible-light telecommunication band: The extinction spectra as a function of wavelength for four nano antenna array chips with length $L = 200\,\text{nm}$, $250\,\text{nm}$, $300\,\text{nm}$, and $350\,\text{nm}$ measured experimentally by using a microspectrophotometer for light polarized perpendicular to the nano-slits arrays. The width is fixed to $w = 50\,\text{nm}$ for all fabricated nano-devices.

2.2. Optical Modulator Metasurface Nano-devices for Near-infrared Telecommunication Band

In addition to visible-light optical modulators based on nano-antenna arrays, in this section, we will demonstrate optical modulators based on subwavelength nano-circuit arrays fabricated on the facet of Nb thin films for operations at near-infrared telecommunication band. The Nb thin film thickness and substrate were selected to be the same as for visible-light modulator devices: a $300\,\text{nm}$ thick sputtered Nb film on a Sapphire substrate of $30\,\text{mm}$ diameter and $0.5\,\text{mm}$ thickness.

A closed-cycle cryogen-free optical cryostat setup was used to accomplish the optical reflectivity measurements at near-infrared telecommunication wavelengths. The experiment was performed by mounting one Nb chip at a time. The arrays were illuminated at normal incidence by using continuous waves (CW) white light, which was focused to around a $30\,\mu\text{m}$ diameter spot on the device's surface. The intensity of the light source was set to low intensity, and a spectrophotometer was used to detect the reflected light and its corresponding extinction spectra $A(\lambda) = 1 - R(\lambda)$. The data were taken for two different incident polarization of the electric field parallel (P_x) and perpendicular (P_y) to the plane of the nano-circuit array [10].

We present data for five chips, each with arrays of nano-circuit gratings. Each array covered a total area of $100 \times 100\,\mu\text{m}^2$. The nano-circuit arrays were fabricated into the Nb film surface using the same FIB machine discussed above. Each array has a groove length $L_x = 100\,\mu\text{m}$, width

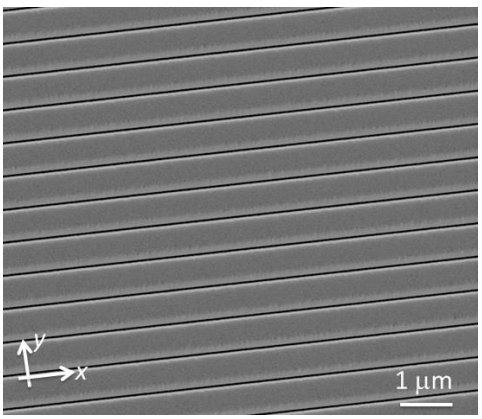

Figure 4: Chip-integrated optical modulators with Nb plasmonic nanocircuit arrays for near-infrared telecommunication band: The top view SEM image of an ultracompact optical modulator device designed for operation at near infrared telecommunication frequencies. The optical modulator is based on Nb nano-circuit array with a width $w = 200\,\text{nm}$, length $L_x = 100\,\mu\text{m}$, and period $P = 900\,\text{nm}$. The optical modulator was manufactured by utilizing FIB milling nanofabrication technology.

$w = 200\,\text{nm}$, and depth $d = 240\,\text{nm}$. The five chips with nano-circuit grating arrays have periods varied from chip to chip: $P = 900\,\text{nm}$, $1000\,\text{nm}$, $1050\,\text{nm}$, $1100\,\text{nm}$, to $1150\,\text{nm}$. Fig. 4 is the SEM image of one device with a width $w = 200\,\text{nm}$, length $L_x = 100\,\mu\text{m}$, and period $P = 900\,\text{nm}$. The image confirms the high-quality fabrication and uniformity of the nano-circuit array [10].

Figure 5 shows the extinction spectra as a function of wavelength $A(\lambda) = 1 - R(\lambda)$ for five nano-circuit grating arrays with periods between $P = 900\,\text{nm}$ and $1150\,\text{nm}$. In Fig. 5(a) the polarization of light is parallel to the device plane (P_x). In this case, we find that the array does not show a strong photoresponse for x-polarized light. On the contrary, a strong photoresponse was observed for y-polarized light, as seen in Fig. 5(b). The plasmonic colours of one nano-grating array with a period $P = 900\,\text{nm}$ are shown to the inset of Fig. 5(a) and Fig. 5(b) for two different light polarization at normal incidence. We observe relatively narrow resonances in the extinction spectra for all five nano-devices for wavelengths longer than the nano-grating period, implying the functionality of the nano-device as a subwavelength metamaterial. We find that the resonances can be tuned to a higher wavelength with the increasing grating period.

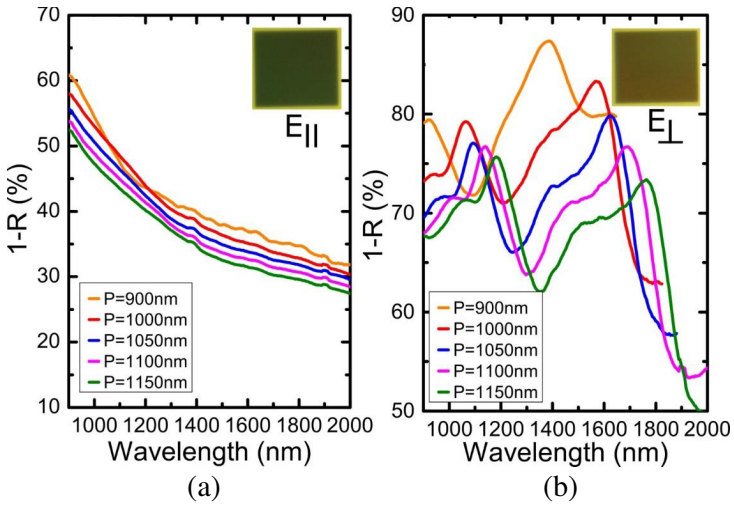

Figure 5: Photo-response of the optical modulators based on Nb nano-circuit arrays in the near infrared telecommunication band: The extinction spectra as a function of wavelength for five chips with nano-circuit arrays. The periodicity of the nanostructures varies between $P = 900\,\text{nm}$ and $1150\,\text{nm}$ for light polarized parallel (a) and perpendicular (b) to the nano circuits arrays, respectively. Insets show the plasmonic colours of one array which has a period $P = 900\,\text{nm}$ for two different polarizations.

3. CONCLUSION

We demonstrated novel ultra-compact and chip-integrated visible to near-infrared light modulators based on nanostructures fabricated on the facet of Nb metallic thin films. At room temperature, our optical modulators offer modulation of light at visible communication bands with a maximum modulation depth MD $\cong 60\%$ at resonant wavelength $\lambda = 716\,\text{nm}$. Moreover, we observe maximum extinction spectra $A(\lambda) = 1 - R(\lambda) \cong 95\%$ at wavelength $\lambda = 650\,\text{nm}$, and $A(\lambda) = 1 - R(\lambda) \cong 88\%$ at resonant wavelength $\lambda = 1380\,\text{nm}$ by engineering the Nb nano-device arrays geometrical parameters. The devices offer tunable plasmonic photo-response between $\lambda = 400\,\text{nm}$ and $\lambda = 2000\,\text{nm}$ (wideband visible to NIR telecommunication wavelengths). Our nano-devices can be integrated with cryogenic superconducting quantum circuits. Given that Nb is a superconducting material with a quantum mechanic phase below their transition temperature ($T_c \cong 9\,\text{K}$) and is widely used as the building block of superconducting quantum circuits and sensors, our results pave the way for the realisation of tunable photonic links, optical interconnects, plasmonic single-photon detectors, ultrasensitive sensors, and bolometers for applications in quantum computing, imaging, and communication.

REFERENCES

1. Arute, F., et al., "Quantum supremacy using a programmable superconducting processor," *Nature*, Vol. 574, 505–510, 2019.

2. Delfanazari, K., R. Puddy, P. Ma, T. Yi, M. Cao, Y. Gul, I. Farrer, D. Ritchie, H. Joyce, M. Kelly, and C. Smith, "On-chip andreev devices: Hard superconducting gap and quantum transport in ballistic Nb-$In_{0.75}Ga_{0.25}As$-Quantum-Well-Nb josephson junctions," *Adv. Mater.*, Vol. 29, No. 37, 1701836, 2017.
3. Pitsun, D., A. Sultanov, I. Novikov, E. Mutsenik, B. Ivanov, A. Matanin, V. Polozov, E. Malevannaya, A. Ivanov, G. Fedorov, K. Delfanazari, I. Rodionov, and E. Il'ichev, "Cross coupling of a solid-state qubit to an input signal due to multiplexed dispersive readout," *Phys. Rev. Applied*, Vol. 14, No. 5, 054059, 2020.
4. Delfanazari, K., R. K. Puddy, P. Ma, T. Yi, M. Cao, C. Richardson, I. Farrer, D. A. Ritchie, H. J. Joyce, M. J. Kelly, and C. G. Smith, "On-chip hybrid superconducting-semiconducting quantum circuit," *IEEE Trans. Appl. Supercond.*, Vol. 28, 1100304, 2018, doi: 10.1109/TASC.2018.2812817.
5. Delfanazari, K., P. Ma, R. Puddy, T. Yi, M. Cao, Y. Gul, C. L. Richardson, I. Farrer, D. A. Ritchie, H. J. Joyce, M. J. Kelly, and C. G. Smith, "Scalable quantum integrated circuits on superconducting two-dimensional electron gas platform," *J. Vis. Exp.*, Vol. 150, e57818, 2019, doi:10.3791/57818.
6. Lecocq, F., F. Quinlan, K. Cicak, J. Aumentado, S. A. Diddams, and J. D. Teufel, "Control and readout of a superconducting qubit using a photonic link," *Nature*, Vol. 591, 575–579, 2021.
7. Usami, K. and Y. Nakamura, "A photonic link for quantum circuits," *Nature Electronics*, Vol. 4, 323—324, May 2021, https://doi.org/10.1038/s41928-021-00587-9.
8. Youssefi, A., I. Shomroni, Y. J. Joshi, N. R. Bernier, A. Lukashchuk, P. Uhrich, L. Qiu, and T. J. Kippenberg, "A cryogenic electro-optic interconnect for superconducting devices," *Nature Electronics*, Vol. 4, 326–332, May 2021, https://doi.org/10.1038/s41928-021-00570-4.
9. Delfanazari, K. and O. L. Muskens, "On-chip visible light communication-band metasurface modulators with niobium plasmonic nano-antenna arrays," arXiv:2107.09939.
10. Delfanazari, K. and O. L. Muskens, "Light-matter interactions in chip-integrated niobium nano-circuit arrays at optical fibre communication frequencies," arXiv:2106.11961.
11. Kalhor, S., S. J. Kindness, R. Wallis, H. E. Beere, M. Ghanaatshoar, R. Degl'Innocenti, M. J. Kelly, S. Hofmann, H. J. Joyce, D. A. Ritchie, and K. Delfanazari, "Active terahertz modulator and slow light metamaterial devices with hybrid graphene superconductor photonic integrated circuits," arXiv:2107.03677.
12. Kalhor, S., M. Ghanaatshoar, H. J. Joyce, D. A. Ritchie, K. Kadowaki, and K. Delfanazari, "Millimeter wave to terahertz compact and low-loss superconducting plasmonic waveguides for cryogenic integrated nano-photonics," arXiv:2106.08594.
13. Kahl, O., S. Ferrari, V. Kovalyuk, G. N. Goltsman, A. Korneev, and W. H. P. Pernice, "Waveguide integrated superconducting single-photon detectors with high internal quantum efficiency at telecom wavelengths," *Sci. Rep.*, Vol. 5, 10941, 2015.
14. Orchin, G. J., D. De Fazio, A. Di Bernardo, M. Hamer, D. Yoon, A. R. Cadore, I. Goykhman, K. Watanabe, T. Taniguchi, J. W. A. Robinson, R. V. Gorbachev, A. C. Ferrari, and R. H. Hadfield, "Niobium diselenide superconducting photodetectors," *Applied Physics Letters*, Vol. 114, No. 25, 251103, 2019.
15. Delfanazari, K, R. A. Klemm, H. J. Joyce, D. A. Ritchie, and K. Kadowaki, "Integrated, portable, tunable, and coherent terahertz sources and sensitive detectors based on layered superconductors," *Proc. IEEE*, Vol. 108, No. 5, 721–734, 2020.
16. Gerrits, T., N. Thomas-Peter, J. C. Gates, A. E. Lita, B. J. Metcalf, B. Calkins, N. A. Tomlin, A. E. Fox, A. L. Linares, J. B. Spring, N. K. Langford, R. P. Mirin, P. G. R. Smith, I. A. Walmsley, and S. W. Nam, "On-chip, photon-number-resolving, telecommunication-band detectors for scalable photonic information processing," *Phys. Rev. A*, Vol. 84, No. 6, 060301, 2011.
17. Delfanazari, K., H. Asai, M. Tsujimoto, T. Kashiwagi, T. Kitamura, T. Yamamoto, M. Sawamura, K. Ishida, C. Watanabe, S. Sekimoto, H. Minami, M. Tachiki, R. A. Klemm, T. Hattori, and K. Kadowaki, "Tunable terahertz emission from the intrinsic josephson junctions in acute isosceles triangular $Bi_2Sr_2CaCu_2O_{8+\delta}$ mesas," *Opt. Express*, Vol. 21, No. 2, 2171, 2013.
18. Hadfield, R. H., "Superfast photon counting," *Nature Photonics*, Vol. 14, No. 4, 201–202, 2020.
19. Korzh, B., et al., "Demonstration of sub-3 ps temporal resolution with a superconducting nanowire single-photon detector," *Nature Photonics*, Vol. 14, 250–255, 2020.
20. Singh, R. and N. Zheludev, "Superconductor photonics," *Nature Photonics*, Vol. 8, 679, 2014.

21. Tsiatmas, A., V. A. Fedotov, F. J. García De Abajo, and N. I. Zheludev, "Low-loss terahertz superconducting plasmonics," *New J. Phys.*, Vol. 14, 115006, 2012.
22. Kalhor, S, M. Ghanaatshoar, T. Kashiwagi, K. Kadowaki, M. J. Kelly, and K. Delfanazari, "Thermal tuning of high-T_c superconducting $Bi_2Sr_2CaCu_2O_{8+\delta}$ terahertz metamaterial," *IEEE Photonics J.*, Vol. 9, No. 5, 1–8, 2017.
23. Fedotov, V. A., A. Tsiatmas, J. H. Shi, R. Buckingham, P. de Groot, Y. Chen, S. Wang, and N. I. Zheludev, "Temperature control of Fano resonances and transmission in superconducting metamaterials," *Opt. Express*, Vol. 18, 9015, 2010.
24. Keller, J., G. Scalari, F. Appugliese, E. Mavrona, S. Rajabali, M. J. Süess, M. Beck, and J. Faist, "High T_c superconducting THz metamaterial for ultrastrong coupling in a magnetic field," *ACS Photonics*, Vol. 5, No. 10, 3977–3983, 2018.
25. Xiong, Y., T. Kashiwagi, R. A. Klemm, K. Kadowaki, and K. Delfanazari, "Engineering the cavity modes and polarization in integrated superconducting coherent terahertz emitters," *2020 45th International Conference on Infrared, Millimeter, and Terahertz Waves (IRMMW-THz)*, 2020, doi: 10.1109/IRMMW-THz 46771.2020.9370587.
26. Singh, R., J. Xiong, A. K. Azad, H. Yang, S. A. Trugman, Q. X. Jia, A. J. Taylor, and H.-T. Chen, "Optical tuning and ultrafast dynamics of high-temperature superconducting terahertz metamaterials," *Nanophotonics*, Vol. 1, 117–123, 2012.
27. Kadowaki, K., T. Kashiwagi, H. Asai, M. Tsujimoto, M. Tachiki, K. Delfanazari, and R. A. Klemm, "Terahertz wave emission from intrinsic Josephson junctions in $Bi_2Sr_2CaCu_2O_{8+\delta}$," *J. Phys.: Conf. Ser.*, Vol. 400, No. 2, 022041, 2012.
28. Kashiwagi, T., K. Deguchi, M. Tsujimoto, T. Koike, N. Orita, K. Delfanazari, R. Nakayama, T. Kitamura, S. Hagino, M. Sawamura, T. Yamamoto, H. Minami, and K. Kadowaki, "Excitation mode characteristics in Bi2212 rectangular mesa structures," *J. Phys.: Conf. Ser.*, Vol. 400, No. 2, 022050, 2012.
29. Tsujimoto, M., T. Yamamoto, K. Delfanazari, R. Nakayama, T. Kitamura, M. Sawamura, T. Kashiwagi, H. Minami, M. Tachiki, K. Kadowaki, and R. A. Klemm, "Broadly tunable subterahertz emission from internal branches of the current-voltage characteristics of superconducting $Bi_2Sr_2CaCu_2O_{8+\delta}$ single crystals," *Phys. Rev. Lett.*, Vol. 108, 107006, 2012.
30. Kashiwagi, T., M. Tsujimoto, T. Yamamoto, H. Minami, K. Yamaki, K. Delfanazari, K. Deguchi, N. Orita, T. Koike, R. Nakayama, T. Kitamura, M. Sawamura, S. Hagino, K. Ishida, K. Ivanovic, H. Asai, M. Tachiki, R. A. Klemm, and K. Kadowaki, "High temperature superconductor terahertz emitters: Fundamental physics and its applications," *Japanese Journal of Applied Physics*, Vol. 51, 010113, 2012, doi: 10.1143/JJAP.51.010113.
31. Tsujimoto, M., T. Yamamoto, K. Delfanazari, R. Nakayama, N. Orita, T. Koike, K. Deguchi, T. Kashiwagi, H. Minami, and K. Kadowaki, "THz-wave emission from inner IV branches of intrinsic Josephson junctions in $Bi_2Sr_2CaCu_2O_{8+\delta}$," *J. Phys: Conf. Ser.*, Vol. 400, No. 2, 022127, 2012.